Bloch Inductance in Small-Capacitance Josephson Junctions

A. B. Zorin

Physikalisch-Technische Bundesanstalt, Bundesallee 100, 38116 Braunschweig, Germany

(Received 17 October 2005; published 24 April 2006)

We show that the electrical impedance of a small-capacitance Josephson junction also includes, in addition to the capacitive term $-i/\omega C_B$, an inductive term $i\omega L_B$. Similar to the known Bloch capacitance $C_B(q)$, the Bloch inductance $L_B(q)$ also depends periodically on the quasicharge, q, and its maximum value achieved at $q = e(\mathrm{mod}\, 2e)$ always exceeds the value of the Josephson inductance of this junction $L_J(\varphi)$ at fixed $\varphi = 0$. The effect of the Bloch inductance on the dynamics of a single junction and a one-dimensional array is described.

DOI: 10.1103/PhysRevLett.96.167001 PACS numbers: 74.50.+r, 03.65.−w, 74.81.Fa, 85.25.Cp

In recent years the Josephson tunnel junctions with small capacitance have been studied extensively. The interest in superconducting circuits with these junctions can be explained by the remarkable quantum behavior of these macroscopic systems. For example, the small-capacitance junctions can transfer individual Cooper pairs and generate Bloch oscillations [1–3]. These circuits can also exhibit a long-time quantum coherence [4,5]. Important potential applications of these effects include the fundamental standard of current [6] and quantum computing circuits [7].

The small-capacitance Josephson junctions are characterized by the finite ratio $\lambda = E_J/E_c$ of the Josephson coupling energy $E_J = (\Phi_0/2\pi)I_c$ (here I_c is the critical current and $\Phi_0 = h/2e$ is the flux quantum) and the charging energy $E_c = e^2/2C$ (C is the junction capacitance). The remarkable feature of these junctions is their nonlinear differential capacitance C_B related to the local curvature of the zero Bloch energy band [1,2],

$$C_B^{-1}(q) = \frac{d^2E_0}{dq^2}, \tag{1}$$

where $E_0(q)$ is the ground state energy of the junction. E_0 periodically (the period is equal to $2e$) depends on the quasicharge $q = \int^t I(t')dt'$ which is a good variable driven by the current source I [see Fig. 1(a)]. Variable q is analog to the quasimomentum of an electron moving in the periodic potential of a crystal lattice. Similar to the Josephson inductance $L_J(\varphi)$, which depends on the classical phase φ in the large junctions ($\lambda \to \infty$), capacitance C_B can also take on both positive and negative values. The property of variation of the Bloch capacitance in a large range was turned to advantage by Averin and Bruder [8] who suggested a switchable capacitive coupling between Josephson charge qubits. Incorporating the nonlinear Bloch capacitance into a tank circuit made it possible to realize a sensitive electrometer [9] and efficient readout of the Cooper-pair-box qubit [10].

Behavior of these circuits is usually described by the junction model comprising solely the Bloch capacitance Eq. (1). Actually, this approach is applicable for the static case or for a sufficiently slow variation of the quasicharge q. In this Letter we show that the small-capacitance junction model should generally include an inductance term [see Fig. 1(b)]. Such a term is proportional to the second time-derivative $\ddot{q} = \dot{I}$, so the corresponding inductance, which we will call the "Bloch inductance," plays the role of the mass for quasicharge q. We evaluate the effect of the Bloch inductance and show that it can be essential even for the single-band motion of the system.

The circuit consisting of a small-capacitance Josephson junction biased by the ideal source of the classical current $I(t)$ is described by the Hamiltonian $H = H_0 + H_I$ [1,2], where the junction's Hamiltonian and the term due to the source are, respectively, equal to

$$H_0 = \frac{Q^2}{2C} - E_J\cos\varphi \quad \text{and} \quad H_I = -\frac{\Phi_0}{2\pi}\varphi I(t). \tag{2}$$

The operator of the charge Q is conjugate to the phase operator φ and is equal to $Q = \frac{2e}{i}\frac{\partial}{\partial\varphi}$ in φ representation. The quasiparticle tunneling is neglected for the sake of clarity. The eigenenergies $E_n(k)$ and the Bloch eigenstates $|k, n\rangle$ of the base Hamiltonial H_0 are periodic functions of the continuous quasi-wave number $k = q/2e$ or the quasicharge q, with the period equal to 1 and $2e$, respectively; the band index $n = 0, 1, 2, \ldots$ [11].

The operator of the phase is given in this basis by the matrix elements [1,2,12]

$$\varphi_{kk'}^{nn'} = i\frac{\partial}{\partial k}\delta(k-k')\delta_{nn'} + \varphi_k^{nn'}\delta(k-k')(1-\delta_{nn'}). \tag{3}$$

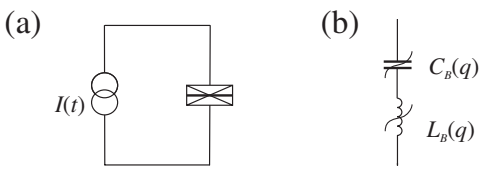

FIG. 1. (a) Electrical diagram of the current-biased small-capacitance Josephson junction and (b) the equivalent circuit of this junction for a small ac signal. Connected in series, the Bloch capacitance C_B and Bloch inductance L_B both depend on the instant value of the quasicharge $q(t) = \int^t I(t')dt'$ which is set by the current source.

 © 2006 The American Physical Society

Since Hamiltonian H is diagonal with respect to the variable k, the density matrix elements $\rho_{kk'}^{nn'}$ take the form $\sigma_{nn'}\delta(k-k')$. After taking trace over this variable, the equation of motion $\dot{\rho} = (1/i\hbar)[H, \rho]$ is reduced to

$$\dot{\sigma}_{nn'} = i\omega_k^{nn'}\sigma_{nn'} + if_I\sum_{n_1=0}^{\infty}[\varphi_k^{nn_1}\sigma_{n_1n'} - \varphi_k^{n_1n'}\sigma_{nn_1}]. \quad (4)$$

Here $\omega_k^{nn'} = [E_n(k) - E_{n'}(k)]/\hbar$ is the interband angular frequency, f_I is the instant Bloch frequency $f_I = I(t)/2e$, and the quasi-wave number time dependence is governed by f_I,

$$k(t) = k(0) + \int_0^t f_I(\tau)d\tau. \quad (5)$$

The operator of voltage, $V = (\Phi_0/2\pi)\dot{\varphi} = (i/2e)\times[H, \varphi]$, is given by the matrix elements [12,13]

$$V_{nn'} = \frac{1}{2e}\frac{\partial E_n}{\partial k}\delta_{nn'} + i\frac{\Phi_0}{2\pi}\omega_k^{nn'}\varphi_k^{nn'}. \quad (6)$$

The diagonal term $V_{00} = V(k)$ gives the voltage value in the ground state [see the plots for a wide range of parameter λ in Fig. 2(b) of Ref. [14]], while its derivative gives the reverse capacitance value C_B^{-1} Eq. (1) shown in Fig. 2(a). The observable value of the voltage is equal to

$$\langle V\rangle = \mathrm{Tr}\{V\rho\} = \sum_{n,n'=0}^{\infty} V_{nn'}\sigma_{n'n}, \quad (7)$$

so the nonzero off-diagonal terms of the voltage operator can also, in principle, contribute to $\langle V\rangle$.

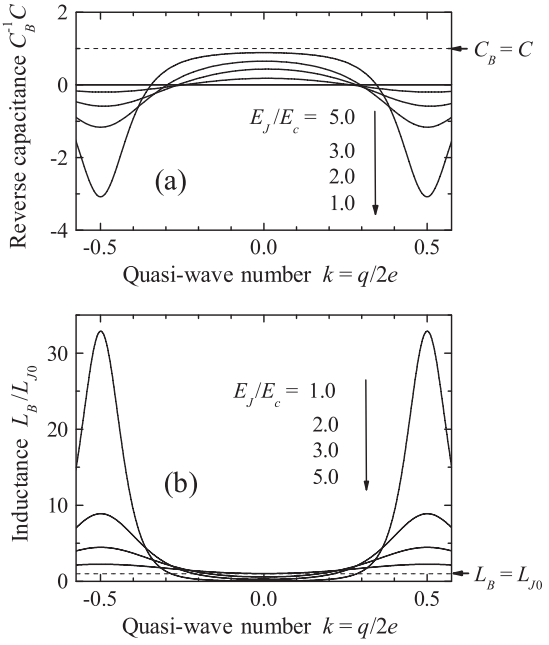

FIG. 2. Normalized reverse Bloch capacitance (a) and Bloch inductance (b) in the zero band (ground state) vs quasicharge for several values of the energy ratio $\lambda = E_J/E_c$.

We solve Eq. (4), taking into account the two lowest bands, i.e., $n, n' = 0$ and 1. We also assume that the excitation to the state $n = 1$ is small, so $\sigma_{00} \lesssim 1$, while $\sigma_{11}, |\sigma_{01}|, |\sigma_{10}| \ll 1$. This assumption is adequate if both the instant Bloch frequency $f_I(t)$ and the maximum rate of its alteration $\dot{f}_I(t)$ are sufficiently small, i.e., the dimensionless parameters $\alpha \equiv \max(f_I)/\Omega_k \ll 1$ and $\alpha_1 \equiv \max(\dot{f}_I)/\Omega_k^2 \ll 1$, where the transition frequency is denoted as $\Omega_k \equiv \omega_k^{10}$. In this case, the solution of the equations of motion

$$\dot{r} \equiv \dot{\sigma}_{00} - \dot{\sigma}_{11} = 2if_I(\varphi_k^{01}\sigma_{10} - \varphi_k^{10}\sigma_{01}), \quad (8)$$

$$\dot{\sigma}_{01} = \dot{\sigma}_{10}^* = -i\Omega_k\sigma_{01} - if_I\varphi_k^{01}r \quad (9)$$

reads

$$r = \sigma_{00} = 1, \qquad \sigma_{11} = 0, \quad (10)$$

$$\sigma_{01}(t) = \sigma_{10}^*(t) = e^{-i\int_0^t\Omega_{k'}dt'}\sigma_{01}(0) - ie^{-i\int_0^t\Omega_{k'}dt'}\int_0^t e^{i\int_0^{t'}\Omega_{k''}dt''}\varphi_{k'}^{01}f_BI(t')dt', \quad (11)$$

where we introduce the quasi-wave numbers $k' = k(t')$ and $k'' = k(t'')$. Keeping the first-order contribution with respect to α and α_1, we finally arrive at

$$\sigma_{01} = Ae^{-i\int_0^t\Omega_{k'}dt'} - \frac{\varphi_k^{01}}{\Omega_k}\left(f_I(t) + i\frac{\dot{f}_I(t)}{\Omega_k}\right). \quad (12)$$

The first term describes the time evolution (oscillations) of the density matrix element due to Hamiltonian H_0. The amplitude A of these high-frequency oscillations depends on the initial conditions, i.e.,

$$A = \sigma_{01}(0) + \frac{\varphi_0^{01}}{\Omega_0}\left(f_I(0) + i\frac{\dot{f}_I(0)}{\Omega_0}\right), \quad (13)$$

where $\varphi_0^{01} \equiv \varphi_k^{01}(t=0)$ and $\Omega_0 \equiv \Omega_k(t=0)$. For the system initially prepared in the ground state, $\sigma_{nn'}(0) = \delta_{n,0}\delta_{0,n'}$, and at "smooth" switching on of the current $I(t)$, i.e., $I(0) = 0$ and $\dot{I}(0) = 0$, the amplitude $A = 0$. The last term on the right-hand side of Eq. (12) is, however, essential, yielding the dependence of σ_{01} on $\dot{f}_I = \ddot{k}$.

The observable value of the voltage Eq. (7) is equal to

$$\langle V\rangle = V_{00}\sigma_{00} + 2\Re(V_{10}\sigma_{01}) = V(q) + \frac{\Phi_0}{\pi}\frac{|\varphi_k^{01}|^2}{\Omega_k}\ddot{k} \quad (14)$$

and can therefore be presented in the form

$$\langle V\rangle = V(k) + L_B(k)\frac{dI}{dt}. \quad (15)$$

Here we introduce the Bloch inductance

$$L_B(k) = \frac{\hbar}{e^2}\frac{|\varphi_k^{01}|^2}{\Omega_k} = 2\frac{E_J}{\hbar\Omega_k}|\varphi_k^{01}|^2L_{J0}, \quad (16)$$

where L_{J0} is the Josephson inductance of a similar classical junction (i.e., in the absence of charging effects, $E_c \to 0$),

taken at zero argument, $L_J(\varphi = 0) = \Phi_0/(2\pi I_c)$. One can see that in contrast to the phase-dependent Josephson inductance $L_J(\varphi)$, the Bloch inductance $L_B(k)$ is a positive periodic function of the quasi-wave number (quasicharge). Physically, L_B still characterizes the kinetic properties of supercurrent which is now the operator [13] whose value depends on the system state, i.e., on the good variable k, or, equivalently, a very wide wave packet over phase φ in φ representation.

Let us consider the behavior of the Bloch inductance at small and large λ. In these limiting cases, the analytical expressions for the matrix elements φ_k^{01} can be taken from Ref. [1]. For $\lambda \ll 1$, inductance L_B increases resonantly in the vicinity of the degeneracy points, i.e.,

$$L_B = L_B^{\max}/(1 + \xi^2)^2, \qquad |\xi| \lesssim 1 \tag{17}$$

at $k = (1 + \lambda\xi)/2(\mathrm{mod}\,1)$. The peak value is equal to $L_B^{\max} = 32\lambda^{-2}L_{J0} \gg L_{J0}$. Outside the resonance region, L_B drops dramatically when approaching $k = 0(\mathrm{mod}\,1)$, the lowest level of $L_B^{\min} = 0.5\lambda^3 L_{J0} \ll L_{J0}$.

At large Josephson couplings, $\lambda \gg 1$, both the interband frequency $\Omega_k \approx \omega_p = (8E_JE_c)^{1/2}/\hbar = (8/\lambda)^{1/2}E_J/\hbar$ (ω_p is the Josephson plasma frequency) and the matrix elements $|\varphi_k^{01}| \approx |\varphi_{\mathrm{osc}}^{01}| = (2/\lambda)^{1/4}$ (equal to those of the equivalent harmonic oscillator) do not depend on k. The Bloch inductance almost takes on the constant value, $L_B \approx L_{J0}$. Taking into account the fact that corrections to $\varphi_{\mathrm{osc}}^{01}$ are exponentially small ($\propto \exp[-(8\lambda)^{1/2}]$) and accounting only for corrections to the oscillator's energy eigenvalues due to anharmonicity of the Josephson potential, the expression for L_B reads

$$L_B(k) = [1 + (2\lambda)^{-1/2}]L_{J0}. \tag{18}$$

For several intermediate values of parameter λ, the inductance L_B is presented by the plots in Fig. 2(b), obtained by numerical methods.

If the dc part of the quasi-wave number $k = q/2e$ is fixed and the small ac part is driven by current $I(t) = I_1 e^{i\omega t}$, the junction voltage according to Eq. (15) is equal to $V = V(q) + Z(\omega)I_1 e^{i\omega t}$. The electrical impedance of the junction $Z(\omega) = i[\omega L_B - (\omega C_B)^{-1}]$ is purely reactive [see Fig. 1(b)]. Thus, at a sufficiently high frequency ω, the inductive term can be appreciable.

At small Josephson couplings, $\lambda \ll 1$, the maximum effect of L_B can be expected to be near the degeneracy points Eq. (17). However, even in these points, the inductive resistance ωL_B approaches the capacitive resistance $-(\omega C_B)^{-1}$ (the positive value due to the negative value of $C_B = -\lambda C/4$) only at $\omega = \Omega_k = E_J/\hbar$, i.e., at the frequency of the interband transition. At such a high frequency, our approach is not applicable. At lower frequencies, the effect of L_B is rather small and can be presented as a frequency-dependent correction to the reverse Bloch capacitance,

$$C_B^{-1} = -\frac{4}{\lambda C} \to -\frac{4}{\lambda C}\left(1 + \frac{\omega^2}{\Omega_k^2}\right), \qquad \omega \ll \Omega_k. \tag{19}$$

Such renormalization of the Bloch capacitance can, in principle, be detected in experiment on the high-frequency Bloch-capacitance-based readout of the Cooper-pair-box qubit [10].

For $\lambda \gg 1$, as follows from the harmonic shape of the eigenenergy $E_0(q)$ [see Eqs. (A3)-(A4) of Ref. [1]], the reverse Bloch capacitance is small,

$$C_B^{-1}(k) = C_{B0}^{-1}\cos(2\pi k), \qquad C_{B0}^{-1} = bB(\lambda)C^{-1}, \tag{20}$$

$$B(\lambda) = \lambda^{3/4}\exp[-(8\lambda)^{1/2}] \ll 1, \tag{21}$$

where the numeric factor $b = \pi^{3/2}2^{11/4} \approx 37$. The maximum (resonance) frequency above which the inductor dominates is

$$\omega_0 = [L_B(0)C_{B0}]^{-1/2} = (bB)^{1/2}\omega_p \ll \Omega_k. \tag{22}$$

Therefore, at least in the range of the frequencies $\omega_0 \lesssim \omega \ll \Omega_k$, the effect of inductance L_B should be significant.

The question arises as to whether the role of the Bloch inductance is essential in the dynamics of an autonomous Josephson junction. For evaluating this effect we introduce a small dissipation by adding to our model Eq. (2) a high-Ohmic resistor, $R \gg R_Q \equiv h/4e^2 \approx 6.45\ \mathrm{k\Omega}$, connected either parallel to the current source in Fig. 1(a) [1,2] or, equivalently, in series with a voltage source V_0, as shown in the inset in Fig. 3. In this case the system is described by a wave packet over k [see Eqs. (71) and (75) of Ref. [1]]. At low temperature, $k_BT \ll \min\{\hbar\Omega_k, [E_0(e) - E_0(0)]\}$, this packet with the center k is sufficiently narrow, $\Delta k \ll 1$. Corresponding interband damping terms in the equation of motion Eq. (9) lead to an exponential decay of the fast-oscillating off-diagonal term $\propto A$ in Eq. (12). Finally, the equation of motion for q takes the form

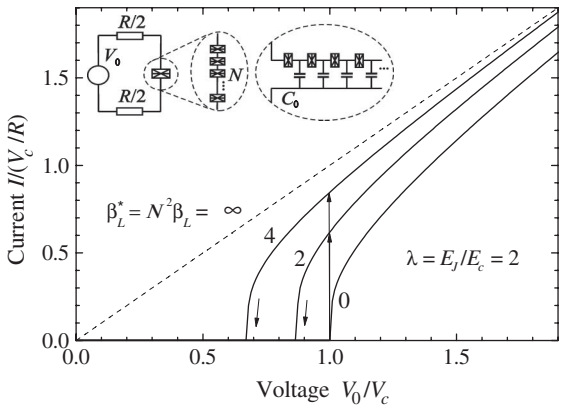

FIG. 3. I-V characteristics obtained in the model including the quasicharge-dependent Bloch inductance Eqs. (23) and (24) for several values of parameter β_L^*. The curves corresponding to the finite values of β_L^* show appreciable hysteresis. The inset shows possible realizations of large values of β_L^*.

$$L_B(q)\ddot{q} + R\dot{q} + V(q) = V_0, \tag{23}$$

or, in dimensionless units,

$$\ell(\theta)\beta_L \frac{d^2\theta}{d\tau^2} + \frac{d\theta}{d\tau} + g(\theta) = \upsilon. \tag{24}$$

Here we introduced $\theta = 2\pi k$, $\tau = \omega_c t$, $\omega_c = V_c/eR$, $\upsilon = V_0/V_c$, $V_c = \max[V(q)]$, and the unity-amplitude periodic function $g(\theta) = V(e\theta/\pi)/V_c$. Parameter $\beta_L = L_{J0}V_c/eR^2$ and the normalized Bloch inductance is $\ell(\theta) = L_B(e\theta/\pi)/L_{J0}$. For large λ, the values of these parameters are $V_c \approx \pi^{-1}eC_{B0}^{-1}$, $\omega_c \approx (RC_{B0})^{-1}$, $g(\theta) \approx \sin\theta$, $\ell(\theta) \approx 1$, and

$$\beta_L \approx \frac{\omega_c^2}{\omega_0^2} = \frac{L_{J0}}{R^2C_{B0}} = \frac{2bB(\lambda)}{\pi^2\lambda}\left(\frac{R_Q}{R}\right)^2 \ll 1, \tag{25}$$

and Eq. (24) takes the form of the equation, describing a driven, damped pendulum or a resistively shunted Josephson junction [15]. Finite values of corresponding McCumber-Stewart parameter, $\beta_L \gtrsim 1$, ensuring the effect of the inductive term on the dc I-V curve (IVC), can therefore not be achieved.

However, the situation changes dramatically in the case of an array of N junctions connected in series in the same network (see the central part of the inset in Fig. 3). The individual junctions of this array are decoupled and described by Eqs. (23)–(25) with replacement $L_B(q) \to NL_B(q)$, $V(q) \to NV(q)$, $V_c \to NV_c$, and $\beta_L \to \beta_L^* = N^2\beta_L$. Note that the maximum resonance frequency ω_0 Eq. (22) does not change. At sufficiently large $N \gg 1$, the effective McCumber-Stewart parameter β_L^* can be made of the order of 1, even for unavoidably large values of R. As a result, the IVC of such an array can exhibit characteristic hysteresis (see Fig. 3).

In experiment, due to the small stray capacitance C_0 of each island of the array to ground (see the rightmost part in the inset in Fig. 3), the number of decoupled junctions N_0 is limited by the size of the Cooper-pair soliton, i.e., $N_0 = (C_{B0}/C_0)^{1/2}$ [16,17]. At $\lambda \gg 1$, this size increases dramatically, so that it can result in hysteretic IVC. A similar effect has been observed repeatedly by the KTH group in long arrays of small Al junctions [see, e.g., [18]], although these arrays were voltage biased, so the quasiparticle tunneling played an important role in those samples.

The concept of the Bloch inductance allows the sine-Gordon equation, describing static Cooper-pair $2e$ solitons in the small-capacitance junction array [16], to be generalized to the nonstationary case. Each junction included in the elementary cell of the array is presented as shown in Fig. 1. Because of the emerging inertial term $L_B\ddot{q}$, the corresponding sine-Gordon equation for the quasicharge describes a persistent motion of the $2e$ solitons.

In conclusion, we introduced the Bloch inductance and described its effect on the quasicharge dynamics in circuits with small-capacitance Josephson junctions. The effect should manifest itself by an effective renormalization of the Bloch capacitance in the vicinity of the degeneracy points of the Cooper-pair boxes and by a hysteretic behavior of the IVCs of long one-dimensional arrays. The Bloch inductance of the Josephson junction included in the variable electrostatic transformer [8] may at $\lambda \gtrsim 1$ result in an interqubit coupling of resonator-mediated type [19]. Finally, similar to the Josephson inductance, the Bloch inductance may be applied in the dispersive quantum nondemolition readout of Josephson qubits [20].

I wish to thank to thank T. Duty, D. B. Haviland, and S. V. Lotkhov for stimulating discussions and G. Schön and D. Esteve for comments. This work was partially supported by the EU through the SQUBIT-2 and EuroSQIP projects.

[1] K. K. Likharev and A. B. Zorin, J. Low Temp. Phys. **59**, 347 (1985).
[2] D. V. Averin, A. B. Zorin, and K. K. Likharev, Zh. Eksp. Teor. Fiz. **88**, 692 (1985) [Sov. Phys. JETP **61**, 407 (1985)].
[3] L. S. Kuzmin and D. B. Haviland, Phys. Rev. Lett. **67**, 2890 (1991).
[4] Y. Nakamura, Yu. A. Pashkin, and J. S. Tsai, Nature (London) **398**, 786 (1999).
[5] D. Vion, A. Aassime, A. Cottet, P. Joyez, H. Pothier, C. Urbina, D. Esteve, and M. H. Devoret, Science **296**, 886 (2002).
[6] K. K. Likharev and A. B. Zorin, IEEE Trans. Magn. **21**, 943 (1985).
[7] Yu. Makhlin, G. Schön, and A. Shnirman, Rev. Mod. Phys. **73**, 357 (2001).
[8] D. V. Averin and C. Bruder, Phys. Rev. Lett. **91**, 057003 (2003).
[9] L. Roschier, M. Sillanpää, and P. Hakonen, Phys. Rev. B **71**, 024530 (2005).
[10] T. Duty, G. Johansson, K. Bladh, D. Gunnarsson, C. Wilson, and P. Delsing, Phys. Rev. Lett. **95**, 206807 (2005).
[11] After replacing the current source I (in fact, the charge source) by a voltage source V_0 with small capacitance C_g connected in series, this model describes the Cooper-pair box. In this case, the quasicharge is equal to the charge on the capacitive gate, i.e., $q = C_gV_0$.
[12] E. M. Lifshitz and L. P. Pitaevskii, *Statistical Physics* (Pergamon Press, New York, 1980), Part 2.
[13] A. B. Zorin, Zh. Eksp. Teor. Fiz. **125**, 1423 (2004) [JETP **98**, 1250 (2004)].
[14] A. B. Zorin, Phys. Rev. Lett. **76**, 4408 (1996).
[15] D. E. McCumber, J. Appl. Phys. **39**, 3113 (1968); W. C. Stewart, Appl. Phys. Lett. **12**, 277 (1968).
[16] D. V. Averin and K. K. Likharev, in *Mesoscopic Phenomena in Solids*, edited by B. L. Altshuler, P. A. Lee, and R. A. Webb (Elsevier, New York, 1991), p. 175.
[17] D. B. Haviland and P. Delsing, Phys. Rev. B **54**, R6857 (1996).
[18] P. Ågren, K. Andersson, and D. B. Haviland, J. Low Temp. Phys. **124**, 291 (2001).
[19] C. Hutter, A. Schnirman, Yu. Makhlin, and G. Schön, cond-mat/0602086.
[20] A. B. Zorin, Physica (Amsterdam) **368C**, 284 (2002).